

Influence of $\text{Ce}^{3+}/\text{Ce}^{4+}$ ratio on phase stability and residual stress field in ceria–yttria stabilized zirconia plasma-sprayed coatings

R. DAL MASCHIO, P. SCARDI, L. LUTTEROTTI

Dipartimento di Ingegneria dei Materiali, Università di Trento, 38050 Mesiano di Povo, Trento, Italy

G. M. INGO

CNR, Istituto di Teoria e Struttura Elettronica, CP 10, Monterotondo Stazione, Rome, Italy

$\text{CeO}_2\text{-Y}_2\text{O}_3$ stabilized zirconia plasma-sprayed coatings have been produced by two different procedures based on different cooling rates. A high cooling rate (HCR) induced the contemporary presence of CeO_2 and Ce_2O_3 , while cooling in calm air (LCR) induced the presence of only CeO_2 . After subjecting the HCR coating, detached from the substrate, to an air thermal treatment, which oxidizes Ce_2O_3 to CeO_2 , a lower thermal expansion coefficient was measured than in the LCR material, and shrinkage was also observed. This behaviour is explained by the phase composition changes induced by the oxidation of ceria.

1. Introduction

In the last decade, substantial effort [1–3] has been devoted to optimize zirconia-based thermal barrier coatings (TBC). Attention has been focused on the role played by the stabilizer oxides in determining thermo-mechanical properties, phase composition and micro-structural aspects. These studies led to the selection of zirconia with a 6–8 wt % yttria content as the primary candidate material in the current state-of-the-art TBCs. Although this material currently provides adequate service performances, in terms of protection and insulation of hot-section jet-engine components, because both the service temperature and strains will be increased, future TBC requirements will be for an increased spallation and corrosion–erosion resistance.

Recently, the stabilization of ZrO_2 by adding CeO_2 in different amounts, ranging between 18 and 26 wt %, has been successfully proposed [4–6]. It was pointed out that with respect to 8 wt % $\text{Y}_2\text{O}_3\text{-ZrO}_2$ material, $\text{CeO}_2\text{-ZrO}_2$ TBCs exhibit an improved thermal shock resistance, a better corrosion resistance against V_2O_5 and SO_2 and a lower thermal conductivity. By way of contrast, a lower phase composition stability has been evinced. In order to overcome this problem, the combined use of CeO_2 and Y_2O_3 as stabilizers could represent a possible compromise solution, ensuring the good features of both stabilizers with a probable synergic effect.

Very recently, in order to obtain a better characterization of this system for TBC applications, Ingo *et al.* [7] showed by means of X-ray photoelectron spectroscopy (XPS) in a 25.5 $\text{CeO}_2\text{-2.5 Y}_2\text{O}_3\text{-72 ZrO}_2$ (wt %) plasma-sprayed TBC, the effect of the deposition temperature on cerium valence states. XPS res-

ults indicated that, as a consequence of the combined effect of the plasma gas, which reduces CeO_2 to Ce_2O_3 , and the deposition temperature, it is possible to induce in the case of low deposition temperature ($\leq 120^\circ\text{C}$) the presence of a large amount of Ce_2O_3 , or to induce the presence of only CeO_2 when the TBC is cooled in calm air. In the present investigation of coatings deposited at different temperatures, the cerium valence state was related both to the phase composition and to the coating thermal expansion behaviour.

2. Experimental procedure

The TBCs were deposited by a commercial air-pressure plasma spray (APS) equipment according to the powder manufacturer's specifications [8]. The starting pre-alloyed powder commercially obtained had the following chemical composition (wt %): CeO_2 25.1, Y_2O_3 2.54, ZrO_2 71, HfO_2 0.985, Na 0.1, Si 753 p.p.m., Al 586 p.p.m.

During and after deposition on to an AISI 316 stainless steel substrate, the TBCs, about 500 μm thick, were either air-cooled rapidly below 120°C using an air-jet blown continuously on to the front face of the coating (high cooling rate, HCR), or they were cooled to room temperature without any forced air-cooling (low cooling rate, LCR). The temperature was evaluated by means of a thermocouple placed in the substrate 1 mm below the surface to be coated.

It is worth noting that a low deposition temperature is currently adopted for minimizing compressive stresses, caused by thermal expansion mismatch between zirconia coating and the substrate during cooling of

the coating after spraying. In order to avoid the misleading influence of residual stress fields due to fabrication among the different coatings, research has been carried out on samples chemically detached from the substrate.

XPS investigation was carried out on a Escalab MkII (VG) spectrometer using $AlK_{\alpha 1,2}$ radiation as the excitation source ($h\nu = 1486.6$ eV). The electron analyser was operated in fixed analyser transmission (FAT) mode by selecting a constant pass energy of 20 eV; under these operating conditions the measured full width at half maximum (FWHM) of the $Ag^0 3d_{5/2}$ line was 1.0 eV. All measurements were performed at pressures lower than 5×10^{-5} Pa in the analysis chamber. The binding energies (BE) were referenced to the Fermi level of the electron analyser and the confidence in the linearity of the BE scale was based upon setting the position of the $Au 4f_{7/2}$ and $Cu 2p_{3/2}$ peaks at 83.8 and 932.5 eV, respectively. Corrections of the energy shift due to the steady state charging effect were accomplished by assuming that the C 1s line, resulting from the ubiquitous surface layer of adsorbed hydrocarbons, lies at 284.6 eV, that the $Zr 3d_{5/2}$ line in ZrO_2 lies at 182.4 eV and that the Ce^{4+} satellite lies at 916.5 eV [7, 9, 10]. The mean value of 182.4 \pm 0.1 eV was obtained with reference to the $Au 4f_{7/2}$ line from evaporated gold on stoichiometric ZrO_2 [7, 11–13], and this value is in good agreement with the literature data [7, 10, 14–16]. The reproducibility of the results, which was tested in three independent samples, was within ± 0.1 eV. This value was also the estimated uncertainty in BE locations.

X-ray diffraction (XRD) measurements were done using a Rigaku rad B/III diffractometer equipped with a graphite curved crystal monochromator in the diffracted beam, using CuK_{α} radiation produced at 40 kV and 30 mA. The angular regions 27° – 33° and 70° – 77° in 2θ , encompassing the (111) and (400) peaks of zirconia polymorphs, respectively, were studied for qualitative and quantitative analysis of the phases present.

Because the XRD spectra showed a very complex overlapping of the peaks of different phases, a peak separation computer program was employed [17]. Well-established structural constraints, such as a fixed ratio between integrated intensities of (400) and (004) peaks of the tetragonal phase, were introduced during the fitting procedure to obtain more reliable solutions. The consistency of results from the peak

separation of the two angular ranges (intensity ratio and peak positions) was also checked. In addition, a statistical hypothesis test was used to control the real presence of each peak [18].

In order to reoxidize fully the HCR sample, simultaneous differential thermal analysis and thermogravimetric analysis (DTA–TGA) were performed on small pieces with a heating rate of 10 K min^{-1} in air up to 600°C . From the oxidation peak temperature (about 240°C), a thermal treatment was performed in a dilatometer at a heating rate of 5 K min^{-1} , an annealing time of 24 h at 340°C and a cooling rate of 2 K min^{-1} to room temperature, for evaluating the thermal expansion on heating and eventual length changes after the oxidation treatment.

3. Results

Table I lists the core level BEs measured in selected elements, and Fig. 1 shows $Ce 3d_{5/2}$ and $Ce 3d_{3/2}$ photoemission spectra obtained in the two samples LCR and HCR. Comparison with literature results

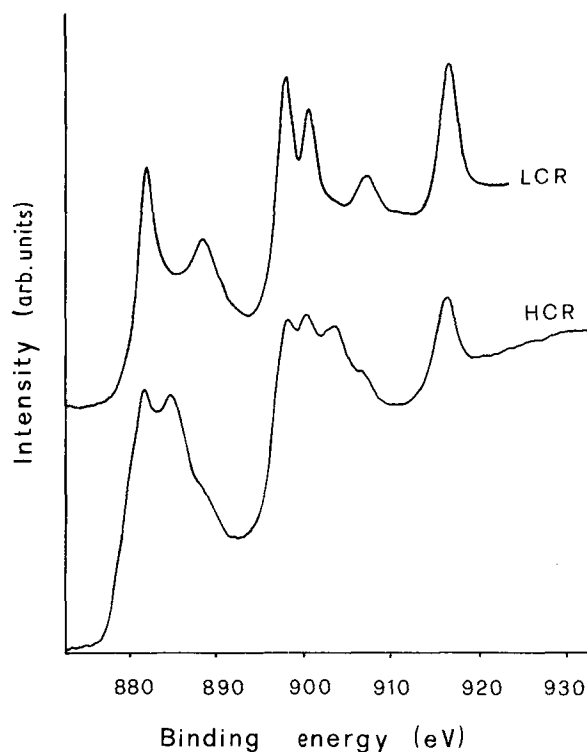


Figure 1 Ce 3d spectra of LCR and HCR samples as-prepared.

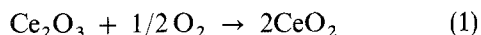
TABLE I Binding energies (BE) for HCR and LCR samples

Sample	Condition	Ce $3d_{5/2}$ (eV)	Ce $3d_{3/2}$ (eV)	Zr $3d_{3/2}$ (eV)	Y $3d_{3/2}$ (eV)	O 1s (eV)
LCR	As-coated	882.2	900.6	182.4	157.2	530.0
		888.7	906.9			532.0
		898.2	916.5			
HCR	As-coated	882.2	900.7	182.4	157.2	529.9
		885.3 ^a	903.7 ^a			531.9
		898.3	916.5			

^a Ce^{3+} component.

and with separate measurements carried out on the starting oxide powder and on the single oxides CeO_2 and Ce_2O_3 , reveals that the surface and fracture surfaces of the LCR sample contain virtually pure CeO_2 , whereas those of the HCR sample show the coexistence of CeO_2 plus Ce_2O_3 species. As far as yttrium, oxygen and zirconium are concerned (Table I), no difference above instrumental uncertainty was apparent between the two samples. The HCR sample after the oxidizing thermal treatment (not reported in Table I and Fig. 1) is very similar to the LCR sample.

From these results it is possible to state that the weight increase evinced in the DTA-TGA analyses on the HCR sample (Fig. 2) is attributable only to Ce^{3+} oxidation according to the reaction



and that the ratio $\text{Ce}^{4+}/\text{Ce}^{3+}$ is about 2. No weight gain nor DTA peak was evident on analysing either the same sample a second time or the LCR sample.

Fig. 3 shows the XRD spectrum of the (111) peak region for an HCR coating, together with the results of peak separation: a superposition of three peaks produces the highly asymmetrical low-angle tail. The fitting of the (400) region shown in Fig. 4a confirmed this result; a tetragonal, T, and two cubic, C_1 and C_2 , zirconia polymorphs were identified.

The low c/a ratio suggests that the tetragonal phase is non-transformable. Further evidence supporting this hypothesis was shown by the XRD spectrum of a ground coating (not reported), to be very similar, within experimental error, to the as-sprayed coating. The contemporary presence of both Y_2O_3 and CeO_2 does not permit good evaluation of the stabilizer content from the peak position by means of the well-known relation between lattice parameters and stabilizer percentage [19]. However, considering the inhomogeneity of the starting powders, where pure

CeO_2 was also present, the C_1 peak in Fig. 4a was attributed to a cerium-rich cubic phase. A value of about 55 mol % CeO_2 can be obtained by comparing the C_1 phase lattice parameter with Tani *et al.*'s data [20]. The lattice parameters and corresponding cell volumes are reported in Table II.

After thermal annealing at 340°C , the C_2 phase is strongly reduced as shown in Fig. 4b with a corresponding increase of T phase. To quantify this variation, integrated intensities of (400) peaks were converted into volume fractions using a modified Miller formulation to account for the presence of two cubic and one tetragonal phase [21]: the results are shown in Table II.

Fig. 5 shows, for comparison, the thermal expansion curves for HCR and LCR samples. It is evident that there is a different behaviour of HCR with respect to LCR up to about 400°C with a thermal expansion coefficient for the former of $6.9 \times 10^{-6}^\circ\text{C}^{-1}$. Above this temperature both samples have a very similar coefficient ($11.8 \times 10^{-6}^\circ\text{C}^{-1}$ for HCR and $11.7 \times 10^{-6}^\circ\text{C}^{-1}$) in the temperature range between 450 and 650°C . Moreover at the end of thermal annealing at 340°C the HCR sample displays a length change, $L/L_0 = -5 \times 10^{-4}$.

4. Discussion

It has already been recognized by some workers that opportune reducing conditions during plasma deposition can change the oxidation degree of zirconia [22]. In our coatings, if quenched by forced air cooling, the cerium ion is also present in the trivalent state, giving rise to high oxygen vacancy concentrations with an increased stability effect. In particular, the presence of Ce_2O_3 tends to stabilize a cubic zirconia with pyrochlore structure [23].

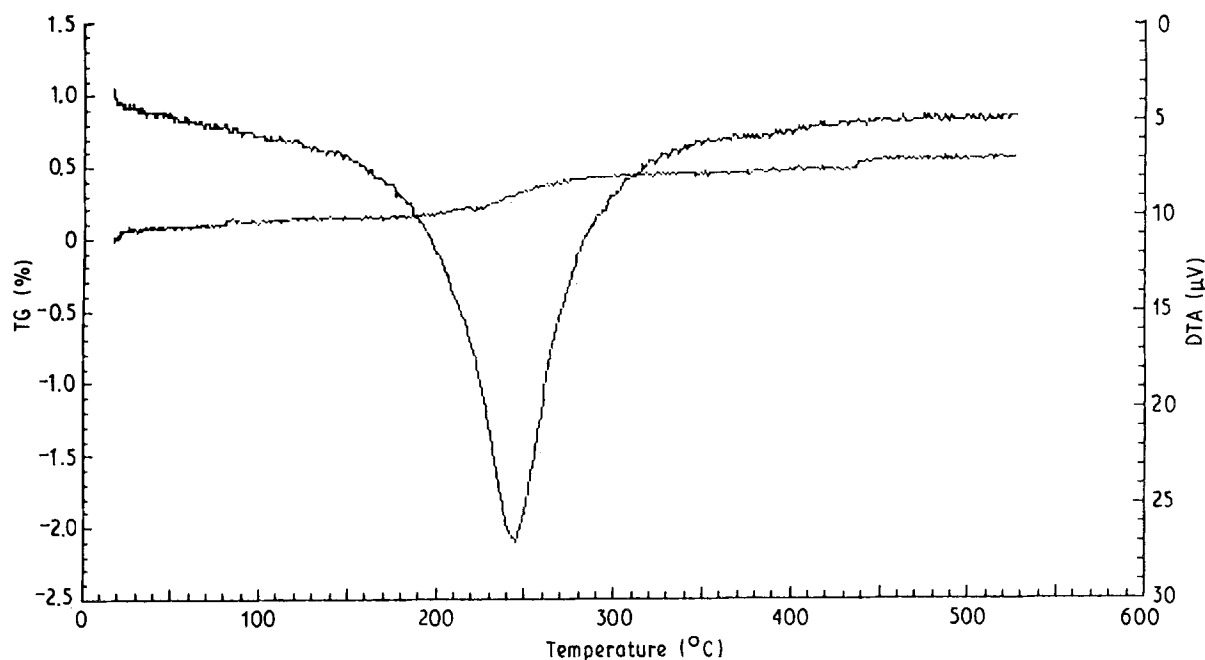


Figure 2 DTA-TGA analyses of the HCR sample as-prepared.

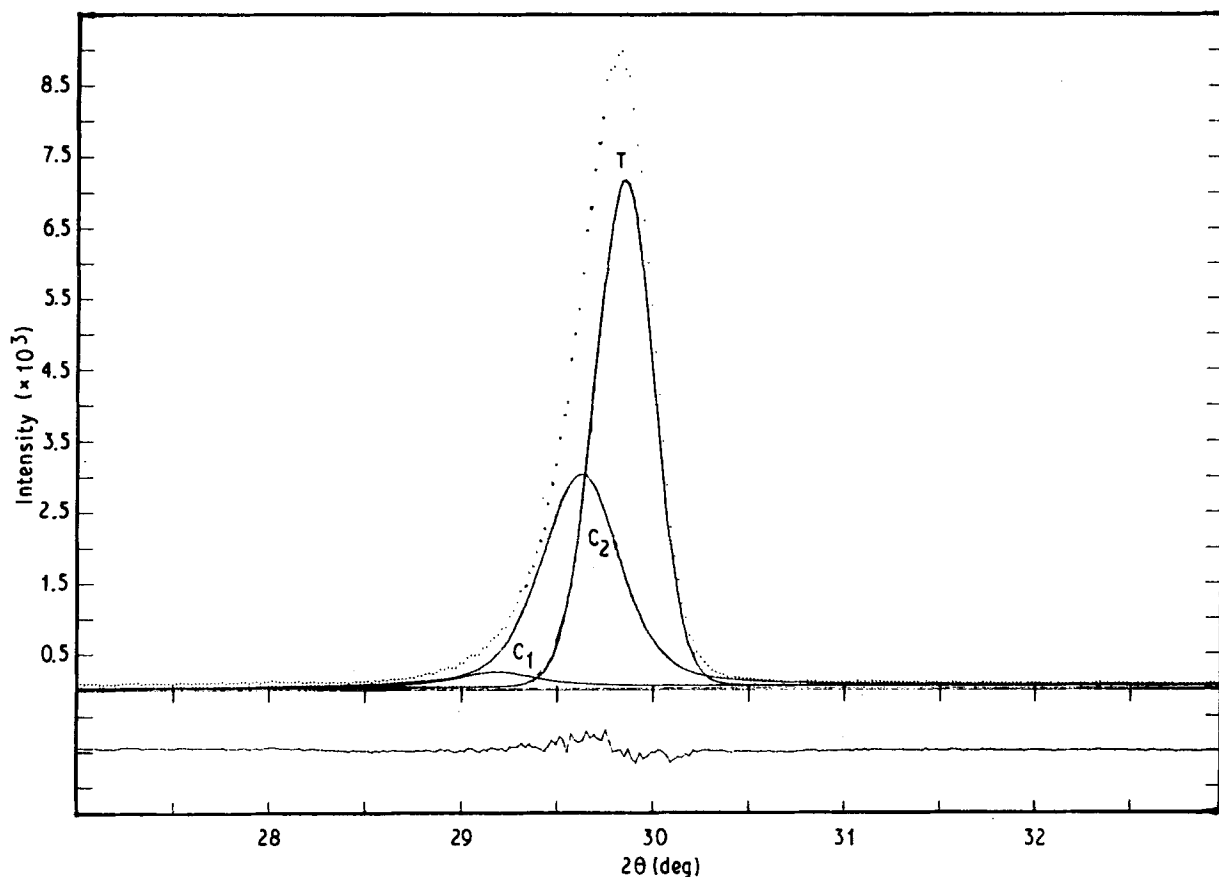


Figure 3 XRD spectrum of the (1 1 1) peak region for an HCR coating (· · ·) as-prepared, and (—) the results of peak separation.

TABLE II Cell parameters and volumetric phase percentages in HCR samples

Phase	Lattice parameters (nm)	Cell volume (nm ³)	Volumetric phase (%)	
			As-prepared	Treated
T	<i>a</i> 0.51486 <i>c</i> 0.52174	0.138 306	62	78
C ₁	<i>a</i> 0.52680	0.146 203	3	3
C ₂	<i>a</i> 0.52053	0.141 042	35	19

The thermal treatment causes complete oxidation, i.e. Ce³⁺ to Ce⁴⁺ transformation, as evinced by XPS spectra, accounting for the weight gain shown by the DTA-TGA analyses.

The cause of the volume change after thermal annealing is less evident. The reason may lie in the change of phase percentage. In fact, the oxidation causes a decrease of oxygen vacancies and a consequent cubic to tetragonal transformation. The increase of tetragonal at the expense of cubic C₂ phase implies a volume diminution; using the data of Table II, the volume change from XRD measurements is $-2.3 \times 10^{-3} \pm 0.7 \times 10^{-3}$, corresponding to an average length change of $-7.7 \times 10^{-4} \pm 2.3 \times 10^{-4}$. The dilatometric length change is -5×10^{-4} in good agreement with the XRD results.

The agreement between the two values, deduced by these completely different techniques, exceeds all expectations, considering the many sources of errors in processing the data. In particular, the concentration of

the two stabilizers in C₂ and T phases influences the structural factors of the present phases, causing possible changes in the constants for quantitative analyses. In order to evaluate the influence of these chemical aspects on the residual stress field in the coatings, we must consider the effect of coating volume shrinkage when the ceramic is bound to the metal substrate.

Within the rough approximations of a uniform stress field in the plane of the coating and a rigid interface between the ceramic coating and the metal substrate, it is possible to make some calculations by means of the elastic solution for a composite sphere, where the core is the metal substrate and the cladding is the ceramic coating [24]. On cooling from the coating deposition temperature, and considering its Young's modulus to be ~ 40 GPa and assuming an elastic behaviour below ~ 900 °C, in LCR samples the ceramic coating is in compression if, during the deposition, the metal substrate exceeds about 400 °C

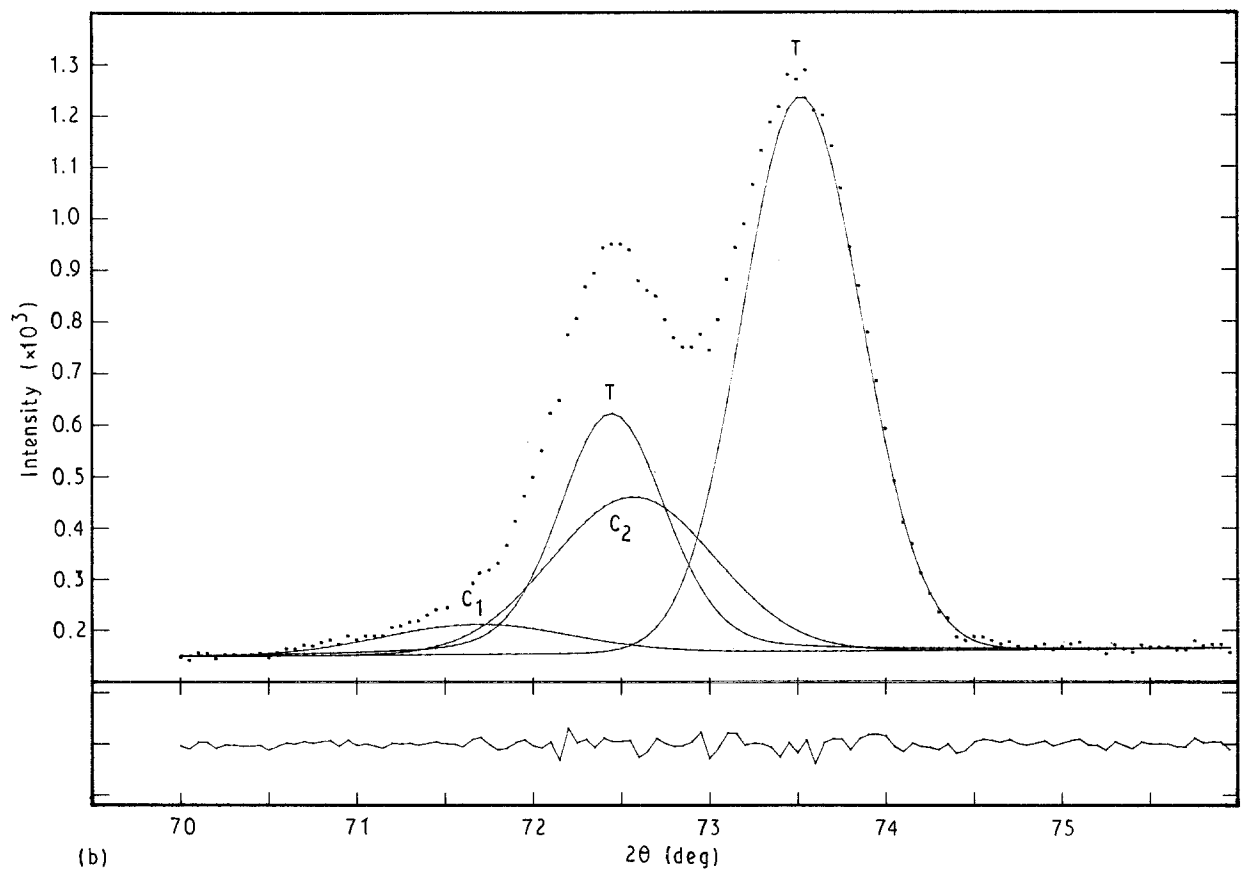
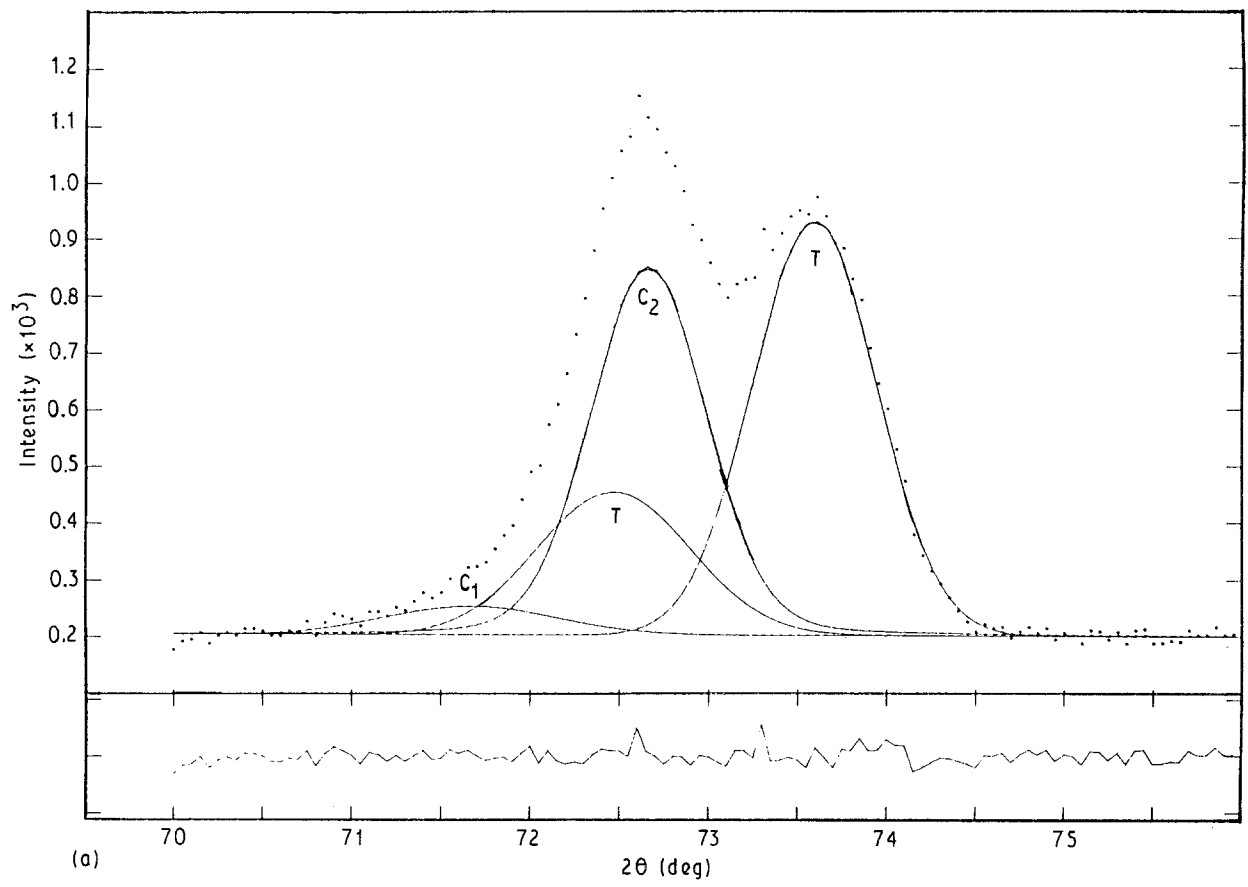


Figure 4 (a) XRD spectra of the (400) peak region for an HCR coating (\cdots) as-prepared; and (—) the results of peak separation. (b) As (a) for (\cdots) an oxidized HCR coating and (—) the results of peak separation.

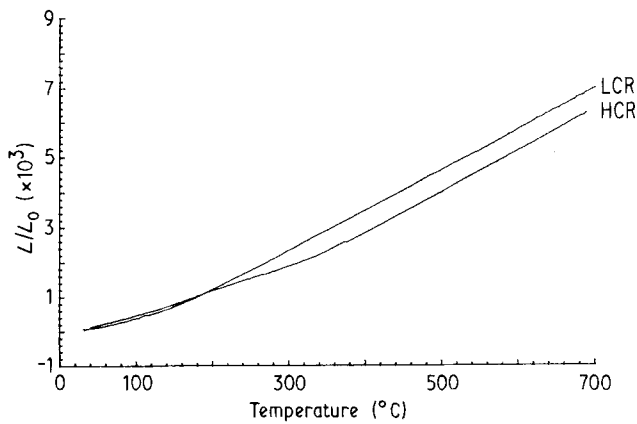


Figure 5 Thermal expansion curves for HCR and LCR coatings as-prepared.

(stainless steel thermal expansion coefficient of about 16×10^{-6}). On the contrary, in HCR samples, a residual tensile stress of ~ 200 MPa is present in the ceramic layer, which is relieved by vertical cracking. Moreover compressive stress is created in the ceramic coating when the metal/ceramic combination is heated from the ceramic side: the ceramic is hotter than the metal, and any attempted thermal expansion of the ceramic is resisted by the more massive metal substrate. In this case the lower thermal expansion of HCR samples with respect to LCR ones, and their shrinkage due to Ce_2O_3 oxidation, are very important in decreasing compressive stresses.

5. Conclusion

$\text{CeO}_2\text{-Y}_2\text{O}_3$ stabilized zirconia plasma-sprayed coatings have been made by two different technological procedures, obtained by changing the cooling system during the deposition. A high cooling rate has been shown to induce the contemporary presence of Ce_2O_3 and CeO_2 , while cooling in calm air induced the presence of only CeO_2 .

On subsequent heating for reoxidation, the HCR coatings, detached from the substrate, showed a lower thermal expansion coefficient than the LCR and, after the oxidation treatment at about 340°C , a shrinkage.

This behaviour has been well explained by the phase composition changes caused by the oxidation of Ce_2O_3 . Moreover, a great influence of the cerium valence state on the residual stress field in the ceramic coating after fabrication and in a subsequent heating has been demonstrated, indicating the linkage be-

tween chemical and technological aspects in plasma-spray deposition.

References

1. R. A. MILLER, *Surf. Coat. Technol.* **30** (1987) 1.
2. T. N. RHYS-JONES, *Corr. Sci.* **6** (1989) 623.
3. T. E. STRANGMAN, *Thin Solid Films* **127** (1985) 93.
4. J. R. BRANDON and R. TAYLOR, *Surf. Coat. Technol.* **39-40** (1989) 143.
5. J. D. REARDON and M. R. DORFMAN, *J. Mater. Energy Systems* **8** (1987) 414.
6. J. W. HOLMES and B. H. PILSNER, in "Proceedings of the National Thermal Spray Conference", edited by D. L. Houck, 14-17 September 1987, Orlando, FL (ASM International, FL, 1987) p. 259.
7. G. M. INGO, E. PAPAARAZZO, O. BAGNARELLI and N. ZACCHETTI, *Surf. Interface Anal.* **16** (1990) 515.
8. METCO, Division of Perkin Elmer, "An Engineering Guide to Coating Performance and Application. METCO 205 NS, Cat. 10-338".
9. T. L. BARR, in "Quantitative Surface Analysis of Materials", ASTM STP 643, edited by N. S. McIntyre (American Society for Testing and Materials, Philadelphia, PA, 1977) p. 83.
10. M. ARFELLI, G. M. INGO and G. MATTOGNO, *Surf. Interface Anal.* **16** (1990) 452.
11. A. E. HUGHES and B. A. SEXTON, *J. Mater. Sci.* **24** (1989) 1057.
12. Y. UWAMINO, T. ISHIZUKA and H. YAMATERA, *J. Electron Spectrosc. Related Phenomena* **23** (1981) 55.
13. C. R. GINNARD and W. M. RIGGS, *Anal. Chem.* **46** (1974) 1306.
14. R. L. TAPPING, *J. Nucl. Mater.* **107** (1981) 151.
15. C. MORANT, J. M. SANZ, L. GALAN, L. SORIANO and F. RUEDA, *Surf. Sci.* **218** (1989) 331.
16. G. M. INGO, *J. Amer. Ceram. Soc.* **74** (1991) 381.
17. A. BENEDETTI, G. FAGHERAZZI, S. ENZO and M. BATTAGLIARIN, *J. Appl. Crystallogr.* **21** (1988) 543.
18. S. ENZO, L. LUTTEROTTI and P. SCARDI, in "Plasma Surface Engineering", edited by E. Broszeit, W. D. Munz, H. Oechsner, K. T. Rie and G. K. Wolf (Deutsche Gesellschaft für Metallkunde, Oberursel, Germany, 1989) p. 799.
19. H. G. SCOTT, *J. Mater. Sci.* **10** (1975) 1527.
20. E. TANI, M. YOSHIMURA and S. SOMIYA, *J. Amer. Ceram. Soc.* **66** (1983) 506.
21. R. A. MILLER, J. L. SMIALEK and R. G. GARLICK, in "Advances in Ceramics", Vol. 3, "Science and Technology of Zirconia", edited by A. H. Heuer and L. W. Hobbs (The American Ceramic Society, Columbus, OH, 1981) p. 241.
22. P. G. ORSINI, R. DAL MASCHIO, F. MARINO and P. SCARDI, in "Zirconia 88", edited by S. Meriani and C. Palmonari (Elsevier, Bologna, 1989) p. 229.
23. K. H. HEUSSNER and N. CLAUSSEN, *J. Amer. Ceram. Soc.* **72** (1989) 1044.
24. G. W. SCHERER, "Relaxation in Glass and Composites" (Wiley, 1986) p. 224.

Received 16 July

and accepted 16 December 1991